

Short communication

Green synthesis of MgO nanoparticles using aqueous leaf extract of Ajwain (*Trachyspermum ammi*) and evaluation of their catalytic and biological activities

Harshal Dabhane^{a,b,*}, Suresh Ghotekar^c, Manohar Zate^d, Sagar Kute^d, Ghanshyam Jadhav^a, Vijay Medhane^{a,e,*}

^a Department of Chemistry, K.R.T. Arts, B.H. Commerce and A.M. Science College, Savitribai Phule Pune University, Nashik 422002, Maharashtra, India

^b Department of Chemistry, G.M.D Arts, B.W Commerce and Science College, Savitribai Phule Pune University, Sinnar 422 103, Maharashtra, India

^c Department of Chemistry, Smt. Devikiba Mohansinhji Chauhan College of Commerce and Science, University of Mumbai, Silvassa 396 230, Dadar and Nagar Haveli (UT), India

^d Department of Physics, G.M.D Arts, B.W Commerce and Science College, Savitribai Phule Pune University, Sinnar 422 103, Maharashtra, India

^e Department of Chemistry, S.V.K.T Arts, Commerce and Science College, Savitribai Phule Pune University, Deolali Camp, Nashik 422401, Maharashtra, India

ARTICLE INFO

Keywords:

Green nanotechnology
MgO NPs
Heterogeneous catalyst
Claisen-Schmidt reaction
Knoevenagel reaction
Biological applications

ABSTRACT

Nanotechnology offers the synthesis of nanoparticles (NPs) with diverse applications in several fields. However, physical and chemical methods were required tedious reaction conditions to attempt the goal, and it is not ecofriendly. Therefore, the green method for nanomaterial synthesis was adapted and successfully used to synthesize nanomaterial using plant extract to overcome these limitations. Herein, we demonstrate a facile, efficient, inexpensive, and green approach for the production of magnesium oxide nanoparticles (MgO NPs) employing Ajwain (*Trachyspermum ammi*) leaf extract, the phytochemicals such as polyphenols and flavonoids present in an extract made possible bio-reduction of $\text{Mg}(\text{NO}_3)_2$. The eco-friendly synthesized MgO NPs were explored by diverse techniques like UV-DRS, FTIR, XRD, PL, BET, BJH, SEM, EDX, and CO_2 -TPD. The peak at 284 nm in UV-DRS confirms the formation of MgO NPs with a band gap of 3.9 eV, whereas the surface area was found to be $12.411 \text{ m}^2/\text{g}$ by BET techniques. Furthermore, the morphology of as-synthesized MgO NPs was confirmed with SEM analysis. The fully characterized MgO NPs were explored as reusable catalysts for Claisen-Schmidt and Knoevenagel reactions and screened for biological activities.

1. Introduction

Nanotechnology is one of the treasured and superb disciplines that serve the top-down and bottom-up approach, which contains physical, chemical, and biological (plant, microorganisms, and biomaterials) methods for synthesizing multifunctional nanomaterials [1–3]. Nanoparticles (NPs) are a multifaceted class of materials that include particulate materials having dimensions 1–100 nm [4]. Those mentioned above physical and chemical techniques are initial time eating, which utilizes excessive energy, the requirement of reducing agents. Also, they are not eco-friendly, which makes them want to discover and innovate

methods that conquer the shortcomings of these chemical and physical methods [5–9]. As evaluated with physical and chemical methods, the biological methods for synthesizing NPs seem pleasant due to their fascinating packages and fewer requirements. It is quick, nontoxic, economical, energy-efficient, and follows the standards of principles of green chemistry [10–16]. Plenty of research was done on synthesizing metal oxide NPs supported by other materials like $\text{g-C}_3\text{N}_4$, which enhances nanomaterial's photocatalytic and biological activity [17–24].

There are numerous reports on the eco-benign production of MgO NPs, and the literature survey suggests that extract of diverse plants and their different parts have been used for the phytogenic fabrication of

Abbreviations: BET, Brunauer-Emmett-Teller; BJH, Barrett-Joyner-Halenda; CO_2 -TPD, Carbon dioxide-temperature programmed desorption; EDX, Energy dispersive X-ray spectroscopy; FTIR, Fourier-transform infrared spectroscopy; MgO-NPs, Magnesium oxide nanoparticles; NPs, Nanoparticles; PL, Photoluminescence; SEM, Scanning electron microscopy; UV-DRS, Ultraviolet visible diffuse reflectance spectroscopy; XRD, X-ray diffraction.

* Corresponding authors at: Department of Chemistry, K.R.T. Arts, B.H. Commerce and A.M. Science College, Savitribai Phule Pune University, Nashik 422002, Maharashtra, India.

E-mail addresses: hadabhane@gmdcollege.in (H. Dabhane), vjmedhane1664@gmail.com (V. Medhane).

<https://doi.org/10.1016/j.inoche.2022.109270>

Received 18 November 2021; Received in revised form 29 January 2022; Accepted 2 February 2022

Available online 5 February 2022

1387-7003/© 2022 Elsevier B.V. All rights reserved.

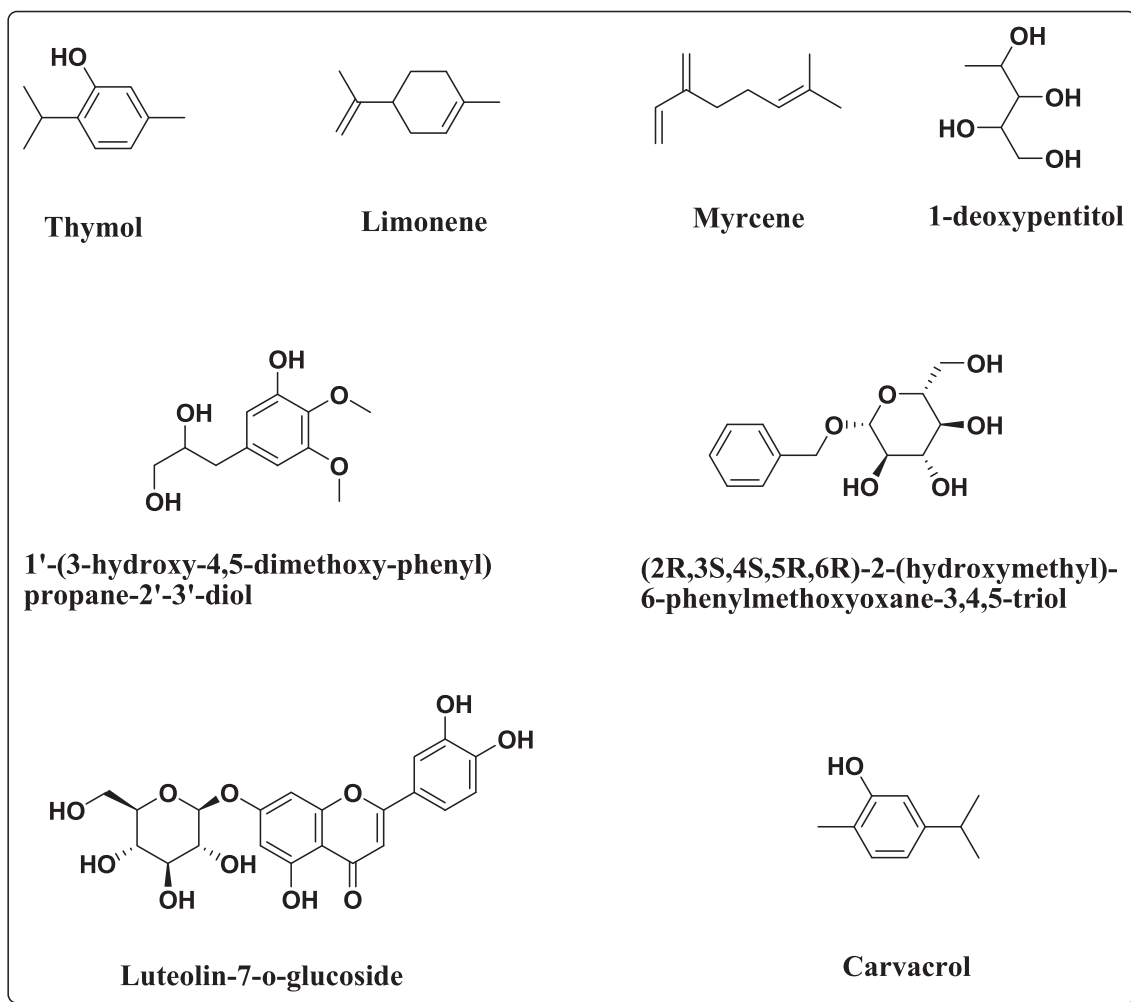
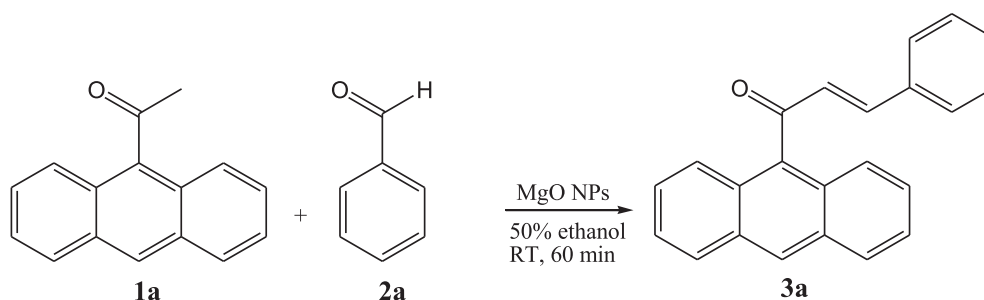
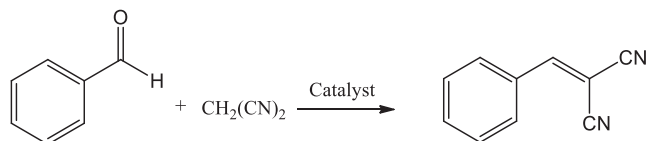


Fig. 1. Active phytochemical constituents in Ajwain.



Scheme 1. Model Claisen-Schmidt reaction of 9-acetylanthracene with benzaldehyde.



Scheme 2. Knoevenagel reaction of an aldehyde with malononitrile.

MgO NPs [25–37]. The MgO NPs possess excellent catalytic activities and are utilized for numerous organic reactions, as evident by literature [38–43]. The exploitation of MgO NPs as a catalyst for various organic transformations is because of their non-toxic nature, high basicity, ready

availability, low cost, and reproducibility [38]. However, besides numerous applications of MgO NPs as a catalyst for organic transformations, the use of MgO NPs synthesized from the plant for organic reactions is not explored to its capacity. Nonetheless, few reports on using plant-mediated MgO NPs for organic reactions [44].

Ajwain (*Trachyspermum ammi*) of the family *Apiaceae*, is an essential therapeutic, spice and aromatic plant. As displayed in Fig. 1, *Trachyspermum ammi* extract contains diverse active bio-compounds, namely thymol, limonene, myrcene, 1'-(3-hydroxy-4,5-dimethoxy-phenyl)propane-2'-3'-diol, Luteolin-7-o-glucoside, and carvacrol [45,46]. Diverse therapeutic uses were noted in the literature for this plant. Further, *Trachyspermum ammi* is also used for pharmacological and biological activities such as antidiarrhoeal, antifungal, insecticidal, antibacterial,

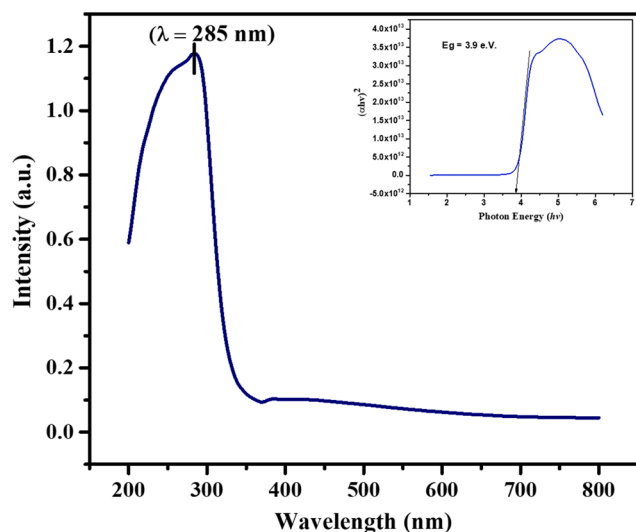


Fig. 2. (a) UV-DRS spectra of Green-MgO NPs (b) Band gap of Green-MgO NPs.

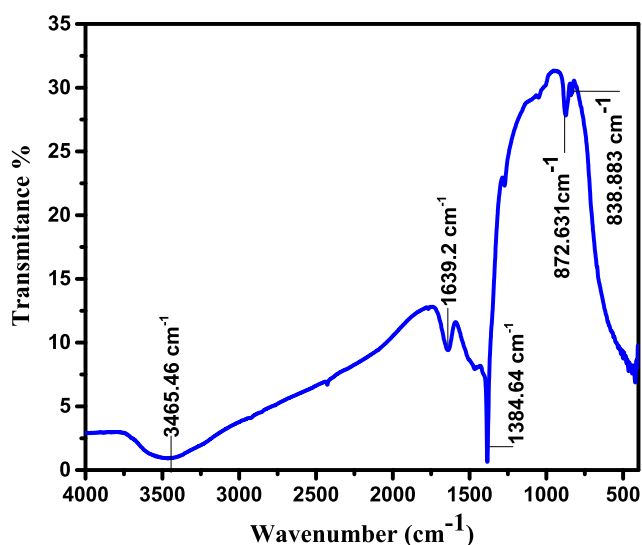


Fig. 3. IR spectra of Green-MgO NPs.

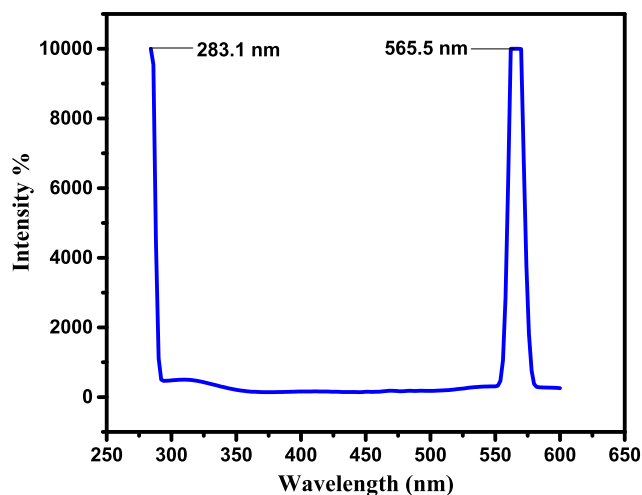


Fig. 4. Photoluminescence spectra of Green-MgO NPs.

antihypertensive, anthelmintic, antispasmodic, nematocidal, anti-inflammatory, anti-lithiasis, anti-nociceptive, antiplatelet-aggregatory, antifilarial, abortifacient, antitussive, enzyme modulation, anti-hyperlipidemic, antioxidant, antiepileptic, and analgesic activity [46,47].

Considering the catalytic potential of plant-mediated MgO NPs, here we first report the green fabrication of MgO NPs employing leaves broth of Ajwain (*Trachyspermum Ammi*) and their use as a catalyst for Claisen-Schmidt and Knoevenagel reactions. The MgO NPs synthesized using the developed protocol were found to show excellent catalytic activities and could be reused up to five times without considerable loss in its catalytic effectiveness for both reactions. In addition, the antimicrobial and antioxidant potential of MgO NPs were also tested, which shows moderate to considerable efficacies compared to standards.

2. Experimental

2.1. Chemical and reagents

All imperative chemicals and reagents of AR grade were purchased from Sigma Aldrich, Mumbai, India, and utilized without additional purification.

2.2. Preparation of Ajwain leaves extract

The fresh leaves of Ajwain (*Trachyspermum ammi*) were collected from Sinnar Tehsil and doubly washed with distilled water (DW). The 10 g of fresh leaves were crushed into tiny pieces and blended into 100 ml of DW, stirred, and then heated at 80 – 95 $^{\circ}\text{C}$ for 30 min. The resulting solution was filtered employing Whatman filter paper and further used to synthesize of MgO NPs.

2.3. Green synthesis of MgO NPs

In a typical process, the freshly prepared extract of Ajwain (*Trachyspermum ammi*) leaves was heated at 60 $^{\circ}\text{C}$, and the pH was kept basic by the addition of 0.1 M NaOH. Next, the hot solution was added magnesium nitrate hexahydrate (1.48 g) slowly, and the resultant mixture was further heated at 60 $^{\circ}\text{C}$ for 15 – 20 min. Later, the reaction mixture was continuously stirred at 25 $^{\circ}\text{C}$ for 2 h. The solid particles were obtained, washed several times with DW followed by alcohol, and finally collected by centrifugation. The obtained solid was then dried in an oven at 70 $^{\circ}\text{C}$ and finally calcinated in a muffle furnace at 300 $^{\circ}\text{C}$ and used for further characterization and applications.

2.4. Characterizations of MgO NPs

The synthesized MgO NPs were explored using diverse spectroscopic and microscopic techniques such as UV spectroscopy by JASCO V-770 spectrophotometer, XRD data was recorded using Model-D8 Advance-Bruker, IR spectra were recorded using FT/IR-4600 type A, and PL spectra using FP-8200 instrument. The topology of synthesized MgO was analyzed by SEM using JSM-6380, and basicity was studied by CO_2 -TPD by BELCAT II Version 0.5.1.10.

2.5. General procedure for the synthesis of chalcone by Claisen-Schmidt reaction

The 9-Acetylanthracene 0.22 g (0.001 mol) and benzaldehyde 0.106 g (0.001 mol) were taken in a 50 ml round bottom (RB) flask, 10 ml of 50% ethanol was used as a solvent with 15 mg MgO NPs as a catalyst. The reaction mixture was stirred in an oil bath at 80 $^{\circ}\text{C}$ for 1 hr. The reaction progress was monitored by TLC method. After completing the reaction, reaction mixture was poured into ice-cold water to separate the product and catalyst (Scheme 1).

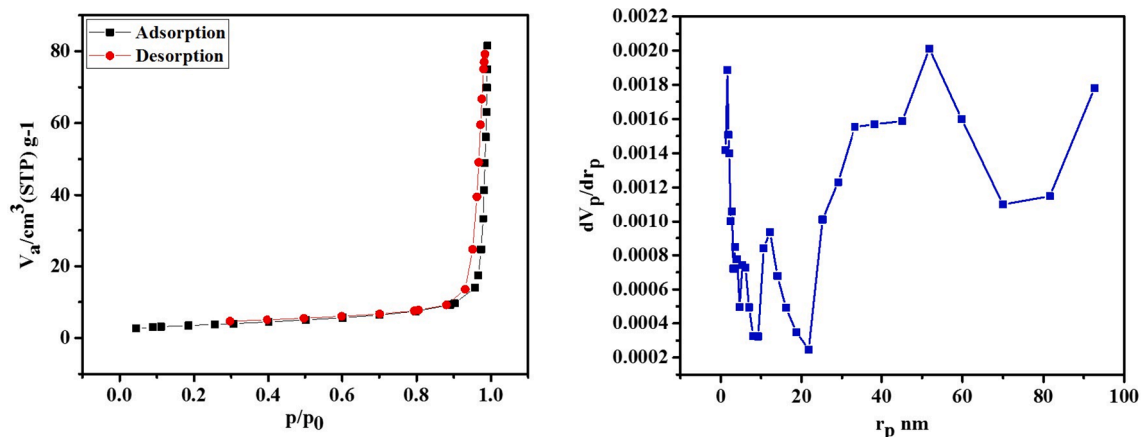


Fig. 5. (a) BET plot of Green-MgO NPs, (b) BJH plot of Green-MgO NPs.

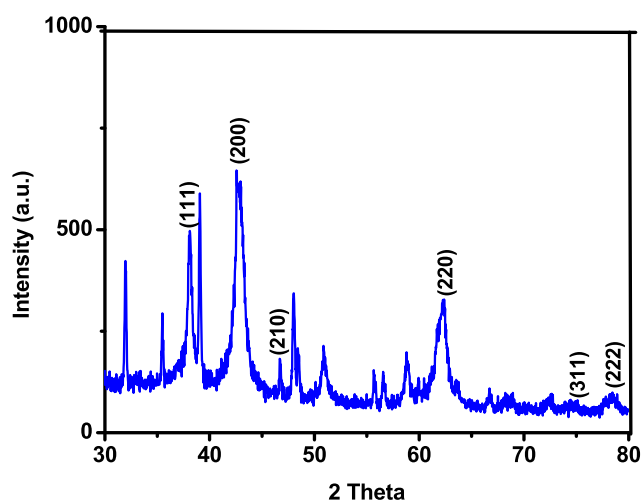


Fig. 6. XRD profile of Green-MgO NPs.

2.6. General procedure for the synthesis of chalcone by Knoevenagel reaction

The benzaldehyde 0.106 g (0.001 mol), malononitrile 0.132 g (0.002 mol), and 15 mg of MgO nanocatalyst was taken in 50 ml RB flask, 10 ml of 50% ethanol was used as a solvent, and the reaction mixture was stirred at room temperature, within a fraction of minute product was obtained. Then, the product was poured into ice-cold water and collected after the filtration (Scheme 2).

2.7. Spectral data of synthesized compounds

This is furnished in the Electronic supplementary data file.

2.8. Antimicrobial activity of MgO NPs

2.8.1. Disk diffusion assay

The antimicrobial efficacy for Ajwain-mediated MgO NPs was performed against four bacterial strains (*B. megaterium*, *B. subtilis*, *S. typhi*, and *E. coli*) and four fungal pathogens (*A. niger*, *P. chrysogenum*, *R. oryzae*, and *C. albicans*) respectively and compared with standard drugs.

This antimicrobial efficacy was conducted following protocol in Dabhane et al. [48].

2.8.2. Resazurin microtiter assay (REMA)

The minimum inhibitory concentration (MIC) was assessed employing the REMA plate assay protocol with few modifications [48]. The concentration ranges used 0.97–500 µg/ml for MgO NPs and standards. The MIC was examined using Fluconazole and Penicillin as positive controls against fungal and bacterial pathogens.

2.9. Antioxidant activity of MgO NPs

The antioxidant performance of eco-benignly fabricated MgO NPs was studied using Hydroxyl (OH) and DPPH radical assay. The detailed protocol for the antioxidant study was reported in our previous study [48].

3. Results and discussion

3.1. Structural and morphological study of MgO NPs

The Ajwain plant facilitated production of MgO NPs was affirmed by UV-visible spectroscopy. The peak at 284 nm in Fig. 2a confirms the formation of MgO NPs. Further, the band gap of eco-friendly synthesized MgO NPs was obtained by intercept line graphically, as shown in Fig. 2b. It was found to be 3.9 eV. Fig. 3 described the FT-IR spectrum of MgO NPs, the broadband at 3465.46 cm⁻¹ indicate the bending vibration of surface hydroxyl group, resulting in either alcoholic or phenolic, moisture adsorption stretching. In contrast, the peaks at 1639.2 cm⁻¹ attributed to a C = C stretching in aromatic compounds and those at 1384.64 cm⁻¹ corresponds to carbonyl stretch in biomolecules present in the plant extract. The stretching vibration appears at 872.63 cm⁻¹, and 838.88 cm⁻¹, indicating the Mg-O bonds. The FTIR results confirm the presence of the bio-molecules in leaf extract of Ajwain (*Trachyspermum ammi*), i.e. flavonoids (Luteolin-7-o-glucoside) and other bio-molecules accountable for the capping and/or stabilization of MgO NPs [49]. The plant-mediated MgO NPs were tested against fluorescence studies and exhibited visible photoluminescence. The fluorescence spectrum is shown in Fig. 4. The enhanced MgO NPs were found to emit two emissions at 283.1 nm and 565.5 nm for excitation at 250 nm. The band gap of biosynthesized MgO NPs was calculated using equation $E = hc/\lambda$, where λ is the highest wavelength taken in fluorescence spectra,

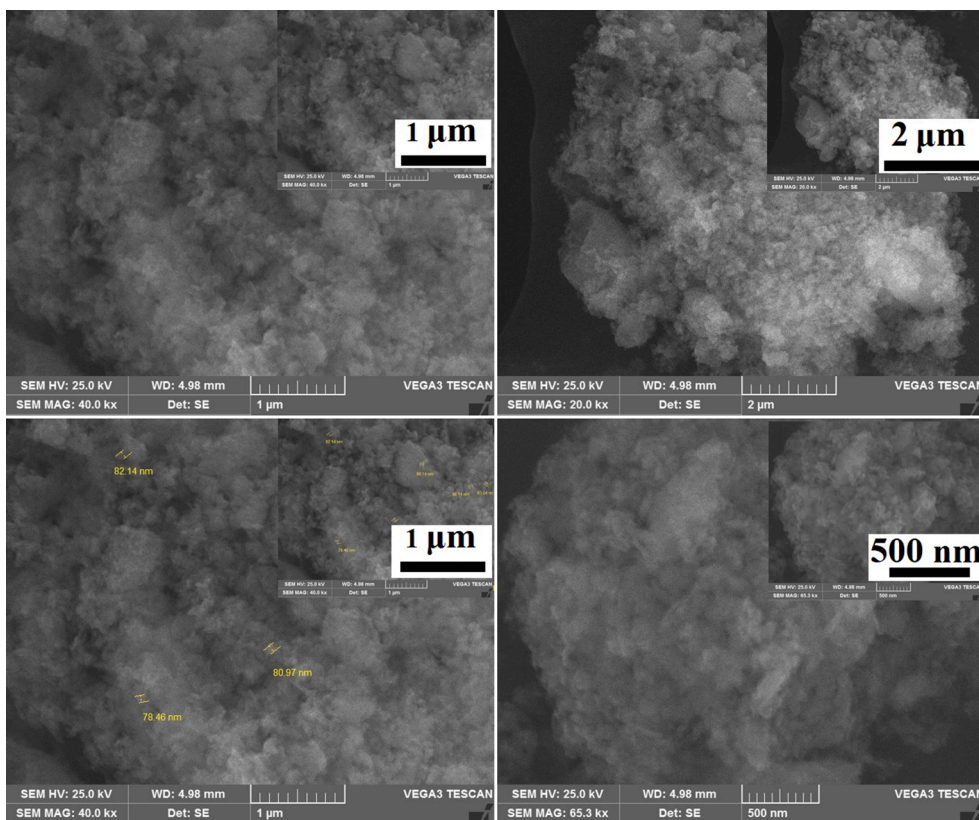


Fig. 7. FE-SEM of Green-MgO NPs.

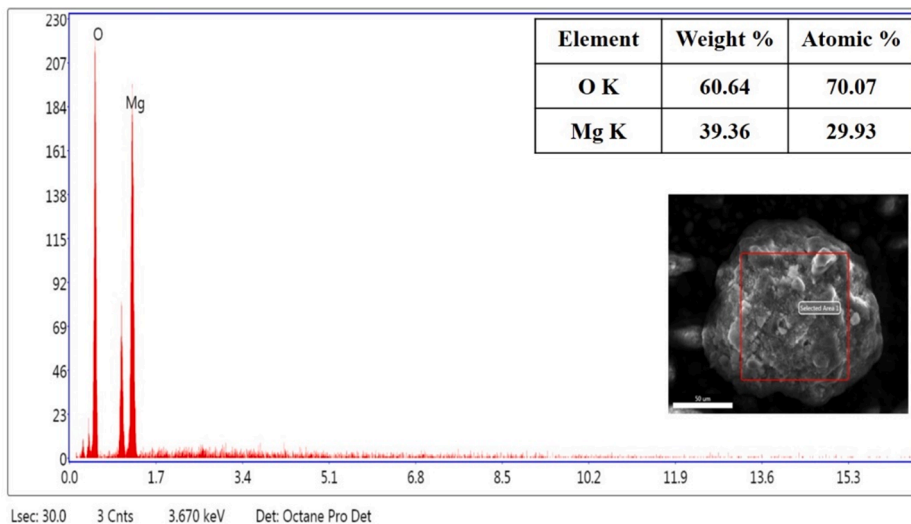


Fig. 8. EDX of green synthesized MgO NPs.

and it was found to be 2.19 eV. The luminescence observed may be due to the availability of phytochemicals or antioxidants in the plant extract.

The catalytic properties of catalysts depend on the surface area and its porosity, large surface area, enhances the catalytic properties of MgO NPs. Fig. 5a represents the BET plot of MgO NPs, the surface area of MgO

NPs measured applying the multipoint BET equation and was found at 12.411 m²/g. In addition, Fig. 5b presents the typical BJH desorption pore sizes distribution curve of MgO NPs. The pour size obtained from peak position was about 51.77 nm, and pore volume was found 0.1201 cm³/g, specifying the moderately small pore size. The BET and BJH

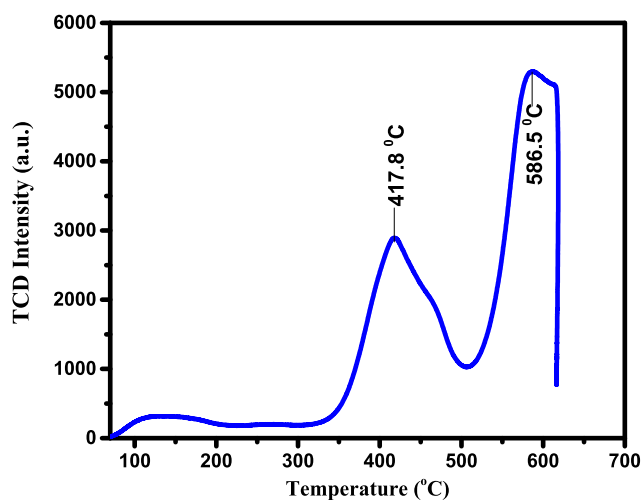


Fig. 9. CO₂-TPD plot of Green-MgO NPs.

curves conclude that most microspores have a size smaller than 51.77 nm.

Fig. 6 displays the XRD pattern of resulting MgO NPs. The XRD profile of MgO NPs synthesized in this study shows six distinct diffraction peaks corresponding to (111), (200), (210), (220), (311), and (222), which confirms hexagonal structure (JCPDS file: 00-004-0823). The XRD pattern reveals that synthesized MgO NPs are polycrystalline, and data were matched previous works [25–26]. In addition, the mean size of MgO NPs was determined from XRD data, which was found to be 83.24 nm. The crystalline size of MgO NPs was ascertained according to Scherrer's equation (1).

$$D = \frac{K\lambda}{\beta \cos \theta} \quad (1)$$

Where, D = Crystalline size

K = 0.9 (Scherrer's constant)

λ = 0.15406 nm (wavelength of X-ray source)

β = FWHM (radians)

θ = Peak position (radians)

Fig. 7 shows representative SEM images that confirm the agglomeration of MgO NPs. The average particle size of MgO NPs revealed by SEM analysis was 78.48 nm. Further, the EDX profile is additional information to affirm the production of MgO NPs. In Fig. 8, the peaks of O and Mg elements in between 0.5 and 1.5 KeV suggest the presence of MgO NPs. The elemental analysis reveals that the percentage of Mg and O element in the material is 39.36 and 60.64 %, respectively.

The basicity of green synthesized MgO NPs using leaf extract of Ajwain (*Trachyspermum ammi*) was studied by CO₂-TPD technique. In the beginning, the material was pre-treated with helium gas from 24 °C to 400 °C for one hour to remove the absorbed moisture and impurities. Then, this material was used for TPD analysis after cooling to room temperature and saturation CO₂ at 50 °C. Finally, the TPD analysis was carried out from 24 °C to 600 °C at a temperature range of 10 °C/min employing helium as inert gas at a 20 cm³/min flow rate. As a result, the amount of CO₂ desorbed from MgO NPs was 420 μ mol/g and 586 μ mol/g, which shows that MgO NPs are more basic in nature (Fig. 9) [50].

3.2. Plausible mechanism for green synthesis of MgO NPs

The MgO NPs were synthesized using leaf extract of Ajwain (*Trachyspermum Ammi*). The phytochemicals study shows the presence of flavonoids, alkaloids, carbohydrates, triterpenoids, tannins, steroids, phenolic compounds, resins, coumarins, saponins, volatile oils, and ascorbic acid as significant phytochemical groups [51]. The phytoconstituents present in leaves extract are accountable for the bio-reduction of magnesium nitrate into MgO NPs (Fig. 10) [52]. In addition, different characterization techniques confirmed the morphology and other properties of MgO NPs.

3.3. Catalytic performance of MgO NPs

The fully characterized MgO NPs were explored as a nano-catalyst for Claisen-Schmidt and Knoevenagel reactions.

The Claisen-Schmidt reaction of 9-acetylanthracene with various

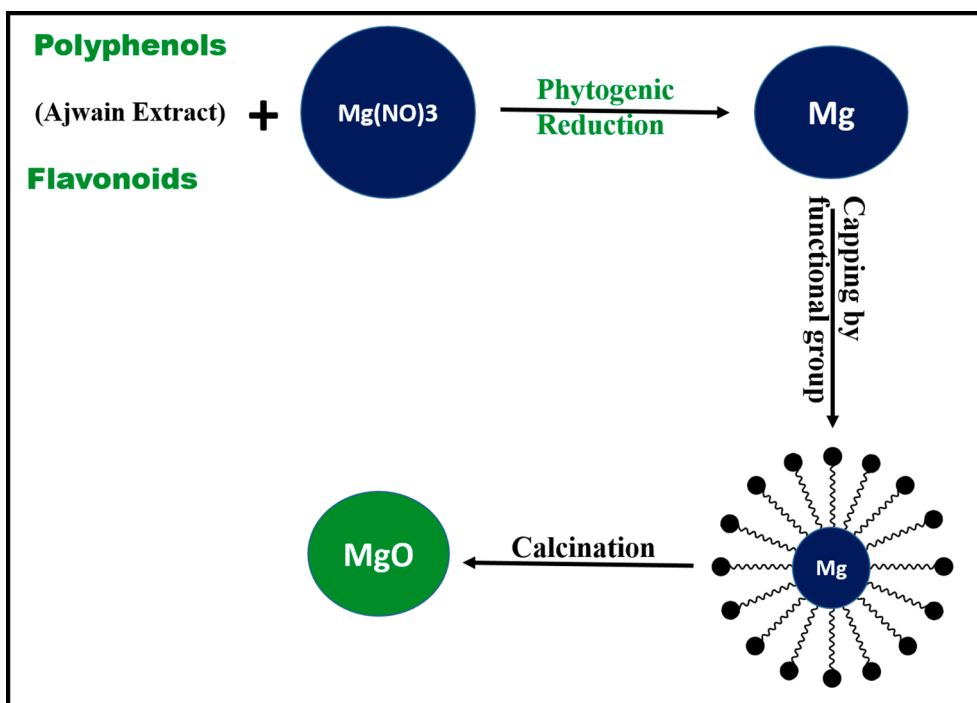


Fig. 10. Possible mechanistic scheme for the bio-reduction of Mg(NO₃)₂ by leaf extract of Ajwain.

Table 1Optimization of reaction conditions for the synthesis of chalcone from 9-acetylanthracene^a.

Entry	Catalyst (mg)	Temperature (°C)	Time (Min.)	Yield (%) ^b
Effect of catalyst loading^c				
1	5	80	60	49
2	10	80	60	68
3	15	80	60	95
4	20	80	60	95
5	25	80	60	95
Effect of time^c				
6	15	80	10	50
7	15	80	20	60
8	15	80	40	65
9	15	80	50	80
10	15	80	60	95
Effect of solvent				
11 ^d	15	80	60	Trace
12 ^e	15	80	60	70
13 ^c	15	80	60	95
14 ^f	15	80	60	90
15 ^g	15	80	60	92

^a Reaction conditions: 9-Acetylanthracene (1 mmol); Benzaldehyde (1 mmol); Temperature (80 °C), Catalyst-MgO NPs, Solvent (10 ml).^b Isolated yield, ^c50% Ethanol, ^dWater, ^e25% Ethanol, ^f75% Ethanol, ^gEthanol.

aldehydes was tested to evaluate MgO NPs catalytic efficiency. Initially, to obtain optimum parameters, the reaction between 9-acetylanthracene and benzaldehyde was considered model reaction (Scheme-1) and the effect of diverse factors like catalyst loading, time, and solvents were screened (Table 1, entries 1–15).

At the outset, we investigated the effectiveness of catalyst loading. The use of 5 mg of a catalyst provides a moderate yield of **3a** (Table 1, entry 1). By the increasing amount of catalyst loading from 5 mg to 15 mg, we observed an increased yield of **3a** (Table 1, entry 2–3). However, with a further increase in the amount of catalyst loading, no notable change in the amount of product was observed (Table 1, entry 4–5). The result shows that 15 mg of MgO NPs catalyst loading is required for the title reaction. Then we carried out the effect of reaction time on reaction outcome, which reveals that there is an increase in yield of expected product (Table 1, entries 6–10). The reaction was found to be complete in 60 min. The effect of solvent on the formation of the product was also checked (Table 1, entries 11–15). A primarily polar solvent like water, ethanol and their mixture were tested. The reaction yielded the product smoothly using 50% ethanol as a solvent (Table 1, entry 13). Hence the optimized reaction parameters were: MgO NPs catalyst (15 mg), solvent: 50% ethanol, temperature: 80 °C, and time: 60 min.

Then optimized reaction parameters were applied for the reaction of 9-acetylanthracene with diverse aldehydes obtaining good to excellent yields of targeted products (Table 2, entries 1–7). Aromatic aldehyde having various groups and aliphatic aldehyde were well tolerated to provide products. The reaction of 9-acetylanthracene with 4-chlorobenzaldehyde and 4-bromobenzaldehyde proceeded smoothly under optimized reaction conditions providing 90 and 81% yield of expected products, respectively (Table 2, entries 2 and 3). The reaction with 2-methoxy benzaldehyde yielded 91% of the product (Table 2, entry 4). Further, the system permits the reaction of sterically hindered aldehydes (2e and 2f), providing excellent yields of anticipated products (Table 2, entries 5–6). Encouraged by these results, 9-acetylanthracene was subjected to react with an aliphatic aldehyde (valeraldehyde) which bestows clean product with 88% yield under optimized reaction conditions (Table 2, entry 7).

The various results on the synthesis of MgO NPs and their results

were discussed in Table 3. Prabhakar et al. reported the Claisen-Schmidt condensation of 9-acetylanthracene and substituted aromatic aldehyde using NaOH as a catalyst in methanol as a solvent. The given reaction condition required 24 h for completion at room temperature, giving an 86% yield (benzaldehyde) [53]. In the current study, we first reported the same reaction in 50% ethanol with green MgO NPs as a catalyst, and the reaction took only 1 h with a high yield (95%). Patil et al. investigated the synthesis of chalcone employing the same reaction in the presence of solar radiation mediated MgO NPs at 140 °C for 4 h under solvent-free conditions [39]. In comparison, Sutradhar et al. reported the condensation reaction between aromatic aldehyde and ketone using synthesized MgO NPs at solvent-free conditions for 4 h [40]. Both reports performed the reaction in solvent-free conditions, but they required a high temperature and longer time to complete, whereas our green route efficiently synthesized MgO NPs in a reaction at 80 °C in 1 h, demonstrating the high basicity of green MgO NPs.

Inspired by the catalytic efficacy of synthesized MgO NPs, we decided to extend its application as a heterogeneous based catalyst for the Knoevenagel reaction of various aldehydes with malononitrile (Scheme 2).

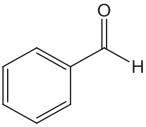
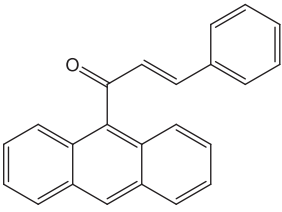
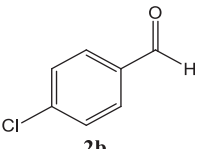
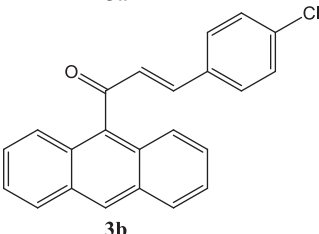
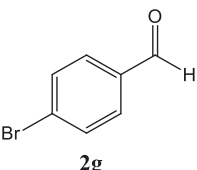
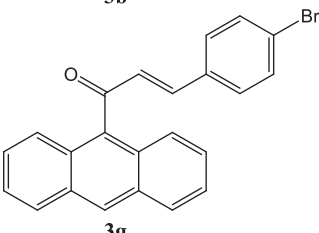
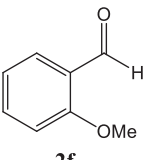
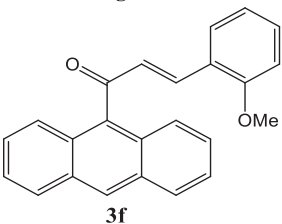
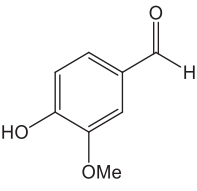
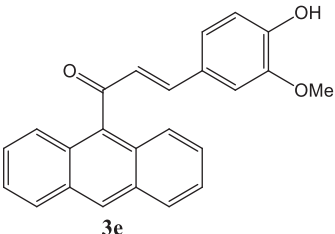
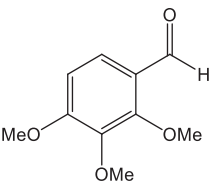
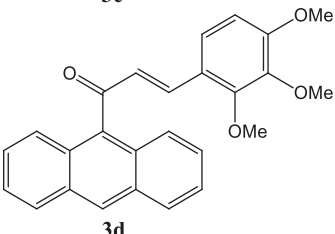
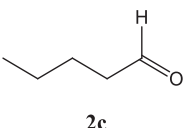
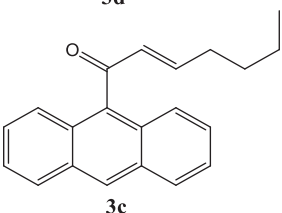
To get the optimum reaction parameters, the reaction between benzaldehyde and malononitrile was chosen as a model reaction, and the influence of diverse parameters such as catalyst loading, temperature, time, and the solvent was tested (Table 4, entries 1–10). Initially, the reaction of malononitrile and benzaldehyde was carried out in the absence of catalyst, which provided traces of product that indicated requisites of the catalyst for the reaction (Table 4, entry 1). The title reaction in the presence of MgO NPs provided the product with excellent yields. To determine the optimum amount of catalyst required to get desired product, reactions were carried out with variable catalyst amounts (5–25 mg) (Table 4, entries 2–6). The reaction with 15 mg catalyst loading was found to be optimum.

Later, the reaction was carried out in water, ethanol, and water–ethanol mixtures (Table 4, entries 7–10). The water was used as a solvent, and the reaction was found to proceed slowly, providing 77 % product in 10 min. However, in ethanol, it gave 90 % product in one minute. Finally, the reaction was found to work smoothly in a 50% water–ethanol mixture providing desired product in just one minute at room temperature. Thus, the optimum reaction parameters for Knoevenagel reaction are benzaldehyde (1 mmol), malononitrile (1.2 mmol), MgO NPs (15 mg), Solvent (50 % ethanol), room temperature, and time (1 min).

To study the advancement and scope of the present protocol, different types of aldehydes containing electron-donating and withdrawing groups were reacted with the active methylene compound (malononitrile) and gave well to excellent yields of the desired product (Table 5). The reaction of malononitrile with aromatic aldehyde bearing –OH, –Cl, –Br, –OMe group was found to yield a significant amount of product (Table 5, entries 2–6). The reaction of vanillin with malononitrile gave the product excellent yield and purity (Table 5, entry 7). The reaction of malononitrile with 2-nitro benzaldehyde also offers product smoothly (Table 5, entry 8). The reaction with cinnamaldehyde and valeraldehyde gives a product with moderate yields under optimized reaction conditions (Table 5, entries 9–10). Finally, the reaction with sterically hindered 2, 3, 4-trimethoxybenzaldehyde provides a product with a good yield (Table 5, entry 11).

The comparative study is shown in Table 6. Roy and co-workers reported the catalytic performance of synthesized nano-crystalline MgO towards Knoevenagel and Claisen-Schmidt condensation reactions. In the given report, Knoevenagel condensation was carried out with aromatic aldehyde and active methylene group with 0.025 g of

Table 2
Claisen-Schmidt reaction of 9-Acetylanthracene with various aldehydes.^a

Entry	Aldehyde	Product (Chalcone)	Yield (%) ^b	Physical constant (°C)
1	 2a	 3a	95	186[53]
2	 2b	 3b	90	156[53]
3	 2g	 3g	81	168[53]
4	 2f	 3f	91	102[53]
5	 2e	 3e	87	143
6	 2d	 3d	91	152
7	 2c	 3c	89	138

^a Reaction condition: 9-acetylanthracene (1 mmol), aldehyde **2a-g** (1 mmol), MgO NPs (15 mg), temperature (80 °C), 50% ethanol (10 ml), time (60 min).

^b Yields of isolated product.

Table 3

Comparative study of Claisen-Schmidt reaction with previous report.

Entry	Mg Precursor	Reducing/ Stabilizing/ Capping agent	Method	Morphology and Size (nm)	Surface Area (m ² /g)	Reaction Condition	% Yield	Ref.
1	Mg(OAc) ₂	1,4-butanediol	Green Method	Spherical (5–20)	–	Solvent Free, 140 °C, 4 h.	98	[39]
2	Mg(NO ₃) ₂	(NH ₄) ₂ CO ₃	Hydrothermal & Solvothermal Method	Different Morphology (6–9)	28–115	Solvent Free, 140 °C, 5 h.	57–99	[40]
3	Mg(OAc) ₂	Ammonium carbonate	Precipitation Method	Nanoflask	–	150 °C, 30 min	99	[42]
4	Mg(NO ₃) ₂	Ajwain plant extract	Green Method	Spherical	51.77	50% ethanol, RT, 60 min	81–95	Present Work

Table 4Effect of reaction parameters on the Knoevenagel reaction are benzaldehyde and malononitrile^a.

Entry	MgO NPs (mg)	Temperature (°C)	Time (Min.)	Yield (%) ^b
Effect of catalyst loading^c				
1	–	25	30	Trace
2	5	25	5	64
3	10	25	5	80
4	15	25	1	98
5	20	25	1	98
6	25	25	1	98
Effect of solvent				
7 ^d	15	70	10	77
8 ^e	15	25	1	90
9 ^f	15	25	1	93
10 ^g	15	25	1	90

^a Reaction conditions: Benzaldehyde (1 mmol); malononitrile (1.2 mmol).^b Isolated yield, ^c50% Ethanol, ^dWater, ^e25% Ethanol, ^f75% Ethanol, ^gEthanol.

nano-crystalline MgO catalyst at solvent-free condition which requiring 25–90 min for completion (yield 84%–98%) [19]. In the present work, we reported the same reaction with an equal amount of catalyst (0.025 g MgO NPs) in 50% ethanol. The reaction is completed in just 1 min and yields higher.

3.4. Recyclability study of MgO NPs

The reusability of the synthesized catalyst was also investigated for Claisen-Schmidt and Knoevenagel reactions. After completion of the reaction, the reaction mixture was filtered, the catalyst was washed with DW followed by alcohol and kept at 300 °C in a furnace for 2 h for activation before the next reaction cycle. The MgO NPs were found to maintain their high effectiveness and selectivity for five consecutive cycles for both reactions (Fig. 11). In addition, there was no considerable loss in yield during the five tested cycles. Thus, the catalyst was successfully recycled, and the reusability protocol was tested up to five times with consistent results.

3.5. Antibacterial efficacy

The bactericidal study of as-prepared MgO NPs was investigated using a well diffusion protocol against gram-positive and negative bacterial strains. The MgO NPs show potent efficacy against gram-positive and negative bacterial strains such as *B. megaterium* and *E. Coli* when compared with positive control Penicillin (Table 7, entries 2 and 3). Although the small size and morphology of green MgO NPs may explain their antibacterial effectiveness. The MIC study also discloses the

considerable antibacterial efficacy, especially against *B. megaterium* and *E. Coli*. Also, the MIC study displays that 125 µg/ml dose of green MgO NPs is sufficient to inhibit the growth of bacterial strains (Table 7, entry 5, and 7).

3.6. Antifungal activity

The antifungal effects of synthesized MgO NPs were tested against fungal strain, and the potent antifungal activity was observed against *A. niger* and *P. chrysogenum* fungal strains (Table 8, entries 1 and 3). Furthermore, the MIC study displays that 250 µg/ml dose of synthesized MgO NPs is sufficient to inhibit the growth of fungal strains (Table 8, entries 5 and 7).

3.7. Antioxidant activity

The antioxidant assay of synthesized MgO NPs is presented in Table 9. In addition, the DPPH radical scavenging performance and OH radical scavenging efficacy were promising compared with standard (ascorbic acid).

4. Conclusion

In summary, we have developed a sustainable protocol for the fabrication of MgO NPs using Ajwain (*Trachyspermum ammi*) leaf extract. These Ajwain leaf extract mediated MgO NPs were explored using UV-DRS, FT-IR, PL, BET, XRD, SEM, and CO₂-TPD analysis. The resulting characterization techniques proved the existence of MgO NPs in the nano range and their basic character, which is suitable for organic transformation. Therefore, synthesized MgO NPs via the phytogenic method was explored as catalysts for Claisen-Schmidt and Knoevenagel reactions. The reactions were optimized concerning various parameters and achieved many products with good to excellent yields. In addition, the catalytic reusability of MgO NPs was also examined and was effectively recyclable for five consecutive cycles without any considerable loss in catalytic performances. Therefore, we conclude that the MgO NPs is the efficient catalyst for organic transformations. Moreover, the MgO NPs were screened for their antimicrobial and antioxidant activities, which showed considerable efficacy compared with standards.

Declaration of Competing Interest

The authors declare that they have no known competing financial interests or personal relationships that could have appeared to influence the work reported in this paper.

Table 5

Knoevenagel reaction of diverse aldehydes with malononitrile.

Entry	Aldehyde	Product	Yield (%) ^b	Physical constant (°C)
1			98	81[54]
2			86	187[55]
3			70	162[54]
4			71	157[55]
5			89	165[55]
6			93	85[54]
7			98	158
8			92	137[55]
9			83	128[54]
10			78	

(continued on next page)

Table 5 (continued)

$ \begin{array}{c} \text{R}-\text{C}_6\text{H}_4-\text{CHO} + \text{CH}_2(\text{CN})_2 \xrightarrow[\text{50\% ethanol, RT}]{\text{MgO NPs}} \text{R}-\text{C}_6\text{H}_4-\text{CH}=\text{C}(\text{CN})_2 \\ \text{4a-4k} \qquad \qquad \qquad \text{5a} \qquad \qquad \qquad \text{6a-6k} \end{array} $				
Entry	Aldehyde	Product	Yield (%) ^b	Physical constant (°C)
11	$ \begin{array}{c} \text{CH}_3(\text{CH}_2)_4\text{CHO} \\ \text{4j} \end{array} $	$ \begin{array}{c} \text{CH}_3(\text{CH}_2)_4\text{CH}=\text{C}(\text{CN})_2 \\ \text{6j} \end{array} $	103	
	$ \begin{array}{c} \text{MeO}-\text{C}_6\text{H}_2(\text{OMe})_3-\text{CHO} \\ \text{4k} \end{array} $	$ \begin{array}{c} \text{MeO}-\text{C}_6\text{H}_2(\text{OMe})_3-\text{CH}=\text{C}(\text{CN})_2 \\ \text{6k} \end{array} $	90	167

^a Reaction conditions: Aldehyde (4a-4 k) (1 mmol); malononitrile (1.2 mmol), 50 % ethanol (10 ml), time (1 min), temperature (25 °C).

^b Isolated yield.

Table 6

Comparative study of Knoevenagel reaction with previous reports.

Entry	Mg Precursor	Reducing/ Stabilizing/ Capping agent	Method	Morphology and Size	Surface Area	Reaction Condition	% Yield	Ref.
1	Mg(OAc) ₂	Ammonium Carbonate	Precipitation Method	Nanoflask	–	Ethanol, 150 °C, 30 min	99	[42]
2	Mg(NO ₃) ₃	NaOH	Precipitation Method	Spherical, 6.04 – 12.83	43.93 – 116.67	Emulsion phase, 30 °C, 30 min	10–87	[43]
3	Mg(NO ₃) ₂	NH ₂ CH ₂ COOH	Solution Combustion Method	Nano-MgO	–	Solvent Free 30 min.	95	[55]
4	Mg(NO ₃) ₂	Ajwain plant extract	Green Method	Spherical	51.77	50% ethanol, RT, 1 min	71–98	Present Work

Catalyst reusability study

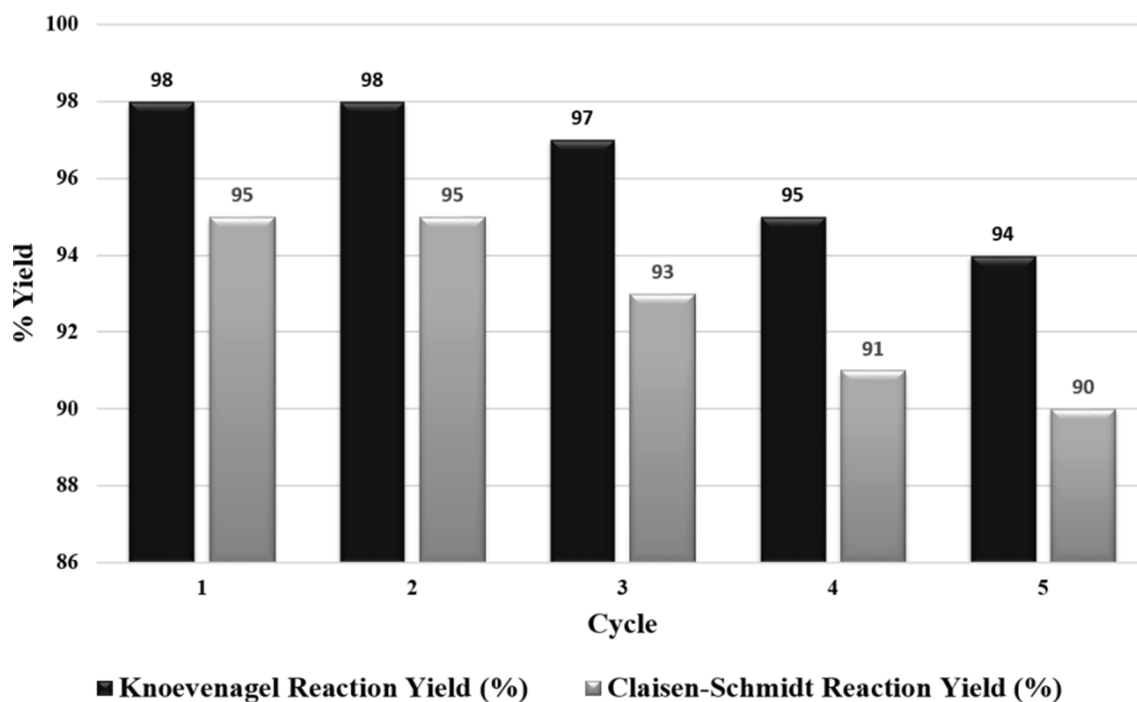


Fig. 11. Catalyst reusability study of MgO NPs.

Table 7

Antibacterial study of MgO NPs against bacterial strains.

Antibacterial activity			
Entry	Bacterial Strain	MgO NPs	Penicillin (Standard)
1	<i>B. subtilis</i>	NZ	+++
2	<i>B. megaterium</i>	++	+++
3	<i>E. coli</i>	++	+++
4	<i>S. typhi</i>	NZ	+++
MIC			
	Bacterial Strain	MgO NPs (µg/ml)	Penicillin (Standard) (µg/ml)
5	<i>B. subtilis</i>	500	1.95
6	<i>B. megaterium</i>	125	3.9
7	<i>E. coli</i>	125	3.9
8	<i>S. typhi</i>	500	1.95

+ = < 5 mm, ++ = >5 & <10 mm, +++ = >10 & < 18 mm, NZ = No zone. Results are the average mean of three parallel experiments.

Table 8

Antifungal study of MgO NPs against fungal strains.

Antifungal activity			
Entry	Fungal Strain	MgO NPs	Fluconazole (Standard)
1	<i>A. niger</i>	++	+++
2	<i>R. oryzae</i>	NZ	+++
3	<i>P. chrysogenum</i>	++	+++
4	<i>C. albicans</i>	NZ	+++
MIC			
	Fungal Strain	MgO NPs (µg/ml)	Fluconazole (Standard) (µg/ml)
5	<i>A. niger</i>	250	1.95
6	<i>R. oryzae</i>	500	1.95
7	<i>P. chrysogenum</i>	250	1.95
8	<i>C. albicans</i>	500	3.9

+ = < 5 mm, ++ = >5 & <10 mm, +++ = >10 & < 18 mm, NZ = No zone. Results are the average mean of three parallel experiments.

Table 9

Antioxidant activities of MgO NPs.

Entry	Material	Antioxidant Activity (%)	
		DPPH	OH
1	MgO NPs	61.4	56.2
2	Ascorbic acid (Standard)	86.4	82.3

Acknowledgements

All persons who have made substantial contributions to the work reported in the manuscript (e.g., technical help, writing and editing assistance, general support), but who do not meet the criteria for authorship, are named in the Acknowledgements and have given us their written permission to be named. If we have not included an Acknowledgement, then that indicates that we have not received substantial contributions from non-authors. This statement is signed by all the authors (a photocopy of this form may be used if there are more than 10 authors): Author's name (typed)

Appendix A. Supplementary data

Supplementary data to this article can be found online at <https://doi.org/10.1016/j.inoche.2022.109270>.

References

- [1] S. Jadoun, R. Arif, N.K. Jangid, R.K. Meena, Green synthesis of nanoparticles using plant extracts: A review, *Environ. Chem. Lett.* 19 (1) (2021) 355–374.
- [2] G.A. Naikoo, M. Mustaqeem, I.U. Hassan, T. Awan, F. Arshad, H. Salim, A. Qurashi, Bioinspired and green synthesis of nanoparticles from plant extracts with antiviral and antimicrobial properties: A critical review, *J. Saudi Chem. Soc.* 25 (9) (2021) 101304, <https://doi.org/10.1016/j.jscs.2021.101304>.

- [3] H.N. Cuong, S. Pansambal, S. Ghotekar, R. Oza, N.T. Thanh Hai, N.M. Viet, V.-H. Nguyen, New frontiers in the plant extract mediated biosynthesis of copper oxide (CuO) nanoparticles and their potential applications: A review, *Environ. Res.* 203 (2022) 111858, <https://doi.org/10.1016/j.envres.2021.111858>.
- [4] G. Guisbiers, S. Mejía-Rosales, F. Leonard Deepak, Nanomaterial properties: size and shape dependencies, *J. Nanomaterials* 2012 (2012) 1–2.
- [5] H. Dabhane, S. Ghotekar, P. Tambade, S. Pansambal, H.C.A. Murthy, R. Oza, V. Medhane, A review on environmentally benevolent synthesis of CdS nanoparticle and their applications, *Environ. Chem. Ecotoxicology* 3 (2021) 209–219.
- [6] H. Dabhane, S.K. Ghotekar, P.J. Tambade, S. Pansambal, H. Ananda Murthy, R. Oza, V. Medhane, Cow Urine Mediated Green Synthesis of Nanomaterial and Their Applications: A State-of-the-art Review, *J. Water Environmental Nanotechnology* 6 (2021) 81–91.
- [7] P. Kumari, P.K. Panda, E. Jha, K. Kumari, K. Nisha, M.A. Mallick, S.K. Verma, Mechanistic insight to ROS and apoptosis regulated cytotoxicity inferred by green synthesized CuO nanoparticles from *Calotropis gigantea* to embryonic zebrafish, *Sci. Rep.* 7 (2017) 1–17.
- [8] S.K. Verma, E. Jha, P.K. Panda, A. Thirumurugan, S. Patro, S.K.S. Parashar, M. Suar, Molecular insights to alkaline based bio-fabrication of silver nanoparticles for inverse cytotoxicity and enhanced antibacterial activity, *Mater. Sci. Eng., C* 92 (2018) 807–818.
- [9] S. Kumari, P. Kumari, P.K. Panda, N. Pramanik, S.K. Verma, M.A. Mallick, Molecular aspect of phytofabrication of gold nanoparticle from *Andrographis paniculata* photosystem II and their in vivo biological effect on embryonic zebrafish (*Danio rerio*), *Environ. Nanotechnol. Monit. Manage.* 11 (2019) 100201, <https://doi.org/10.1016/j.enmm.2018.100201>.
- [10] G. Sharma, R. Soni, N.D. Jasuja, Phytoassisted synthesis of magnesium oxide nanoparticles with *Swertia chirayaita*, *Journal of Taibah University for Science* 11 (3) (2017) 471–477.
- [11] S. Ghotekar, S. Pansambal, M. Bilal, S.S. Pingale, R. Oza, Environmentally friendly synthesis of Cr2O3 nanoparticles: Characterization, applications and future perspective—a review, *Case Studies Chem. Environ. Eng.* 3 (2021) 100089, <https://doi.org/10.1016/j.csee.2021.100089>.
- [12] P.K. Panda, P. Kumari, P. Patel, S.K. Samal, S. Mishra, M.M. Tambuwala, A. Dutt, K. Hilscherová, Y.K. Mishra, R.S. Varma, M. Suar, R. Ahuja, S.K. Verma, Molecular nanoinformatics approach assessing the biocompatibility of biogenic silver nanoparticles with channelized intrinsic steatosis and apoptosis, *Green Chem.* (2022), <https://doi.org/10.1039/D1GC04103G>.
- [13] S.K. Verma, P.K. Panda, P. Kumari, P. Patel, A. Arunima, E. Jha, S. Husain, R. Prakash, R. Hergenröder, Y.K. Mishra, R. Ahuja, R.S. Varma, M. Suar, Determining factors for the nano-biocompatibility of cobalt oxide nanoparticles: proximal discrepancy in intrinsic atomic interactions at differential vicinage, *Green Chem.* 23 (9) (2021) 3439–3458.
- [14] S.K. Verma, E. Jha, B. Sahoo, P.K. Panda, A. Thirumurugan, S.K.S. Parashar, M. Suar, Mechanistic insight into the rapid one-step facile biofabrication of antibacterial silver nanoparticles from bacterial release and their biogenicity and concentration-dependent in vitro cytotoxicity to colon cells, *RSC Adv.* 7 (64) (2017) 40034–40045.
- [15] P. Kumari, P.K. Panda, E. Jha, N. Pramanik, K. Nisha, K. Kumari, N. Soni, M. A. Mallick, S.K. Verma, Molecular insight to in vitro biocompatibility of phytofabricated copper oxide nanoparticles with human embryonic kidney cells, *Nanomedicine* 13 (19) (2018) 2415–2433.
- [16] R. Eram, P. Kumari, P.K. Panda, S. Singh, B. Sarkar, M.A. Mallick, S.K. Verma, Cellular Investigations on Mechanistic Biocompatibility of Green Synthesized Calcium Oxide Nanoparticles with *Danio rerio*, *J. Nanotheranostics* 2 (1) (2021) 51–62.
- [17] R. Monsef, M. Ghiyasiyan-Arani, M. Salavati-Niasari, Design of Magnetically Recyclable Ternary Fe2O3/EuVO4/g-C3N4 Nanocomposites for Photocatalytic and Electrochemical Hydrogen Storage, *ACS Applied Energy Materials* 4 (1) (2021) 680–695.
- [18] H. Safardoust-Hojaghan, M. Salavati-Niasari, O. Amiri, S. Rashki, M. Ashrafi, Green synthesis, characterization and antimicrobial activity of carbon quantum dots-decorated ZnO nanoparticles, *Ceram. Int.* 47 (4) (2021) 5187–5197.
- [19] M. Ghanbari, M. Salavati-Niasari, Copper iodide decorated graphitic carbon nitride sheets with enhanced visible-light response for photocatalytic organic pollutant removal and antibacterial activities, *Ecotoxicol. Environ. Saf.* 208 (2021) 111712, <https://doi.org/10.1016/j.ecoenv.2020.111712>.
- [20] D. Ghanbari, M. Salavati-Niasari, M. Sabet, Preparation of flower-like magnesium hydroxide nanostructure and its influence on the thermal stability of poly vinyl acetate and poly vinyl alcohol, *Compos. B Eng.* 45 (1) (2013) 550–555.
- [21] M. Salavati-Niasari, A. Sobhani, F. Davar, Synthesis of star-shaped PbS nanocrystals using single-source precursor, *J. Alloy. Compd.* 507 (2010) 77–83.
- [22] M. Salavati-Niasari, F. Davar, M.R. Lohman-Estarki, Controllable synthesis of thioglycolic acid capped ZnS (Pn) 0.5 nanotubes via simple aqueous solution route at low temperatures and conversion to wurtzite ZnS nanorods via thermal decompose of precursor, *J. Alloy. Compd.* 494 (2010) 199–204.
- [23] M. Salavati-Niasari, Nanoscale microreactor-encapsulation 14-membered nickel (II) hexamethyl tetraaza: synthesis, characterization and catalytic activity, *J. Mol. Catal. A: Chem.* 229 (2005) 159–164.
- [24] M. Salavati-Niasari, Zeolite-encapsulation copper (II) complexes with 14-membered hexaaza macrocycles: synthesis, characterization and catalytic activity, *J. Mol. Catal. A: Chem.* 217 (2004) 87–92.
- [25] K. Karthik, S. Dhanuskodi, S.P. Kumar, C. Gobinath, S. Sivaramakrishnan, Microwave assisted green synthesis of MgO nanorods and their antibacterial and anti-breast cancer activities, *Mater. Lett.* 206 (2017) 217–220.

- [26] R. Dobrucka, Synthesis of MgO nanoparticles using *Artemisia abrotanum* herba extract and their antioxidant and photocatalytic properties, *Iranian Journal of Science and Technology, Transactions A, Science* 42 (2018) 547–555.
- [27] J. Jeevanandam, Y. San Chan, M.K. Danquah, Biosynthesis and characterization of MgO nanoparticles from plant extracts via induced molecular nucleation, *New J. Chem.* 41 (2017) 2800–2814.
- [28] B. Das, S. Moumita, S. Ghosh, M.I. Khan, D. Indira, R. Jayabalan, S.K. Tripathy, A. Mishra, P. Balasubramanian, Biosynthesis of magnesium oxide (MgO) nanoflakes by using leaf extract of *Bauhinia purpurea* and evaluation of its antibacterial property against *Staphylococcus aureus*, *Mater. Sci. Eng., C* 91 (2018) 436–444.
- [29] A.A. Oladipo, O.J. Adeleye, A.S. Oladipo, A.O. Aleshinloye, Bio-derived MgO nanopowders for BOD and COD reduction from tannery wastewater, *J. Water Process Eng.* 16 (2017) 142–148.
- [30] A. Jain, S. Wadhawan, V. Kumar, S. Mehta, Colorimetric sensing of Fe³⁺ ions in aqueous solution using magnesium oxide nanoparticles synthesized using green approach, *Chem. Phys. Lett.* 706 (2018) 53–61.
- [31] J. Jeevanandam, Y. San Chan, Y.H. Ku, Aqueous *Eucalyptus globulus* leaf extract-mediated biosynthesis of MgO nanorods, *Applied, Biol. Chem.* 61 (2018) 197–208.
- [32] K. Ramanujam, M. Sundrarajan, Antibacterial effects of biosynthesized MgO nanoparticles using ethanolic fruit extract of *Embllica officinalis*, *J. Photochem. Photobiol., B* 141 (2014) 296–300.
- [33] J. Suresh, G. Pradheesh, V. Alexramani, M. Sundrarajan, S.I. Hong, Green synthesis and characterization of hexagonal shaped MgO nanoparticles using insulin plant (*Costus pictus* D. Don) leave extract and its antimicrobial as well as anticancer activity, *Adv. Powder Technol.* 29 (2018) 1685–1694.
- [34] L. Umaralikhan, M.J.M. Jaffar, Green synthesis of MgO nanoparticles and its antibacterial activity, *Iranian J. Sci. Technol. Trans. A Sci.* 42 (2018) 477–485.
- [35] K. Jhansi, N. Jayarambabu, K.P. Reddy, N.M. Reddy, R.P. Suvarna, K.V. Rao, V. R. Kumar, V. Rajendar, Biosynthesis of MgO nanoparticles using mushroom extract: effect on peanut (*Arachis hypogaea* L.) seed germination, *3, Biotech* 7 (2017) 1–11.
- [36] S.K. Moorthy, C. Ashok, K.V. Rao, C. Viswanathan, Synthesis and characterization of MgO nanoparticles by Neem leaves through green method, *Mater. Today: Proc.* 2 (2015) 4360–4368.
- [37] Y. Abdallah, S.O. Ogunyemi, A. Abdelazez, M. Zhang, X. Hong, E. Ibrahim, A. Hossain, H. Fouad, B. Li, J. Chen, The green synthesis of MgO nano-flowers using *Rosmarinus officinalis* L. (Rosemary) and the antibacterial activities against *Xanthomonas oryzae* pv. *oryzae*, *Biomed Res. Int.* 2019 (2019) 1–8.
- [38] H. Dabhane, S. Ghotekar, P. Tambade, S. Pansambal, R. Oza, V. Medhane, MgO nanoparticles: synthesis, characterization, and applications as a catalyst for organic transformations, *European J. Chemistry* 12 (2021) 86–108.
- [39] A.B. Patil, B.M. Bhanage, Novel and green approach for the nanocrystalline magnesium oxide synthesis and its catalytic performance in Claisen-Schmidt condensation, *Catal. Commun.* 36 (2013) 79–83.
- [40] N. Sutradhar, A. Sinhamahapatra, S.K. Pahari, P. Pal, H.C. Bajaj, I. Mukhopadhyay, A.B. Panda, Controlled synthesis of different morphologies of MgO and their use as solid base catalysts, *J. Phys. Chem. C* 115 (2011) 12308–12316.
- [41] S.-W. Bian, Z. Ma, Z.-M. Cui, L.-S. Zhang, F. Niu, W.-G. Song*, Synthesis of Micrometer-Sized Nanostructured Magnesium Oxide and Its High Catalytic Activity in the Claisen–Schmidt Condensation Reaction, *J. Phys. Chem. C* 112 (39) (2008) 15602.
- [42] B. Roy, A.S. Roy, A.B. Panda, S.M. Islam, A.P. Chattopadhyay, Nano-structured Magnesium Oxide as Efficient Recyclable Catalyst for Knoevenagel and Claisen-Schmidt Condensation Reactions, *ChemistrySelect* 1 (15) (2016) 4778–4784.
- [43] A.L. Sadgar, T.S. Deore, R.V. Jayaram, Pickering interfacial catalysis—Knoevenagel condensation in magnesium oxide-stabilized Pickering emulsion, *ACS Omega* 5 (21) (2020) 12224–12235.
- [44] S.K. Sharma, A.U. Khan, M. Khan, M. Gupta, A. Gehlot, S. Park, M. Alam, Biosynthesis of MgO nanoparticles using *Annona squamosa* seeds and its catalytic activity and antibacterial screening, *Micro & Nano Lett.* 15 (1) (2020) 30–34.
- [45] B. Chauhan, G. Kumar, M. Ali, A review on phytochemical constituents and activities of *Trachyspermum ammi* (L.) Sprague fruits, *Am. J. Pharmtech. Res.* 2 (2012) 329–340.
- [46] K. Chahal, K. Dhaliwal, A. Kumar, D. Kataria, N. Singla, Chemical composition of *Trachyspermum ammi* L. and its biological properties: A review, *J. Pharmacognosy Phytochemistry* 6 (2017) 131–140.
- [47] H.M. Asif, S. Sultana, N. Akhtar, A panoramic view on phytochemical, nutritional, ethanobotanical uses and pharmacological values of *Trachyspermum ammi* Linn, *Asian Pacific J. Tropical Biomedicine* 4 (2014) S545–S553.
- [48] H. Dabhane, M. Zate, R. Bharsat, G. Jadhav, V. Medhane, A novel bio-fabrication of ZnO nanoparticles using cow urine and study of their photocatalytic, antibacterial and antioxidant activities, *Inorg. Chem. Commun.* 134 (2021), 108984.
- [49] R.A. Hassan, W.A. Tawfik, L.M. Abou-Setta, The flavonoid constituents of *Leucaena Leucocephala* growing in Egypt, and their biological activity, *Afr. J. Tradit. Complement. Altern. Med.* 11 (2014) 67–72.
- [50] A.L. Gajengi, T. Sasaki, B.M. Bhanage, Mechanistic aspects of formation of MgO nanoparticles under microwave irradiation and its catalytic application, *Adv. Powder Technol.* 28 (2017) 1185–1192.
- [51] A.A. Qureshi, K.E. Kumar, Phytochemical constituents and pharmacological activities of *Trachyspermum ammi*, *Plant Archives* 10 (2010) 955–959.
- [52] N.A.N. Mohamad, N.A. Arham, J. Jai, A. Hadi, Plant extract as reducing agent in synthesis of metallic nanoparticles: a review, *AMR* 832 (2014) 350–355.
- [53] M. Prabhakar, T. Merry, S. Tsurho, R. Zatsu, N. Jain, A. Sataniya, S. Enaganti, Synthesis, characterization and biological evaluation of 9-anthracenyl chalcones as anti-cancer agents, *J. Chem. Pharm. Res.* 9 (2017) 185–192.
- [54] F. Hajizadeh, B. Maleki, F.M. Zonoz, A. Amiri, Application of structurally enhanced magnetite cored polyamidoamine dendrimer for Knoevenagel condensation, *J. Iran. Chem. Soc.* 18 (4) (2021) 793–804.
- [55] J. Hameeda, G. Chandrappa, M. Pasha, Nano-Mgo/bulk-MgCl₂: An efficient catalyst for Knoevenagel condensation, *Catalyst* 25 (2013) 0C.